Neuron, Vol. 18, 827–838, May, 1997, Copyright ©1997 by Cell Press

Association and Stoichiometry of K_{ATP} Channel Subunits

John P. Clement IV,* Kumud Kunjilwar,* Gabriela Gonzalez,* Mathias Schwanstecher,† Uwe Panten,† Lydia Aguilar-Bryan,‡ and Joseph Bryan*

*Department of Cell Biology
Baylor College of Medicine
Houston, Texas 77030

†Department of Medicine
Baylor College of Medicine
Houston, Texas 77030

‡Institut für Pharmakologie und Toxikologie
Braunschweig
Federal Republic of Germany

Summary

ATP-sensitive potassium channels (K_{ATP} channels) are heteromultimers of sulfonylurea receptors (SUR) and inwardly rectifying potassium channel subunits ($K_{IR}6.x$) with a $(SUR–K_{IR}6.x)_4$ stoichiometry. Association is specific for $K_{IR}6.x$ and affects receptor glycosylation and cophotolabeling of $K_{IR}6.x$ by ^{125}I-azidoglibenclamide. Association produces digitonin stable complexes with an estimated mass of 950 kDa. These complexes can be purified by lectin chromatography or by using Ni^{2+}–agarose and a his-tagged SUR1. Expression of $SUR1{\sim}(K_{IR}6.2)_i$ fusion constructs shows that a 1:1 SUR1:$K_{IR}6.2$ stoichiometry is both necessary and sufficient for assembly of active K_{ATP} channels. Coexpression of a mixture of strongly and weakly rectifying triple fusion proteins, rescued by SUR1, produced the three channel types expected of a tetrameric pore.

Introduction

ATP-sensitive potassium channels are found in diverse cell types, including pancreatic β cells, brain, heart, and skeletal and smooth muscle cells, where they are thought to couple metabolism to membrane electrical activity (Noma, 1983; Misler et al., 1986; Ashcroft, 1988). The conductance of these channels is inhibited by ATP and activated by MgADP. In pancreatic β cells, where their function is best understood, K_{ATP} channels set the resting membrane potential and serve as a critical electrical connection between blood glucose concentration and insulin secretion. When glucose metabolism increases, the decrease in intracellular [ADP] reduces K_{ATP} channel activity, resulting in cell depolarization, activation of voltage-gated L-type Ca^{2+} channels, and Ca^{2+}-induced insulin secretion (reviewed by Aguilar-Bryan and Bryan, 1996). Mutations that disturb β cell K_{ATP} channel function cause persistent hyperinsulinemic hypoglycemia of infancy (PHHI) (Thomas et al., 1995b; Kane et al., 1996; Dunne et al., 1997), an autosomal recessive disease of newborns characterized by constitutive insulin secretion despite severe hypoglycemia. The PHHI susceptibility gene(s) map to human chromosome 11p15.1 (Glaser et al., 1994; Thomas et al., 1995a), the locus of both SUR1 and $K_{IR}6.2$. Mutations in either subunit have been shown to cause PHHI (Thomas et al., 1995b; Nestorowicz et al., 1996a, 1996b; Thomas et al., 1996), confirming that these subunits comprise the β cell K_{ATP} channel. The gene-mapping data indicate that the two K_{ATP} channel subunits are clustered in this region, and we have shown that SUR1 is located approximately 4.5 kb 5′ of $K_{IR}6.2$ (Aguilar-Bryan and Bryan, 1996). Their proximity on chromosome 11 argues for the possibility that the receptor and K_{IR} might have evolved from a single ancestral gene.

Reconstitution of K_{ATP} channels indicates they are a novel structural class of ion channels, requiring both a member of the small inward rectifier potassium channel family, either $K_{IR}6.1$ (uKATP, ubiquitous KATP) or $K_{IR}6.2$ (BIR, β cell inward rectifiers), plus a sulfonylurea receptor, SUR1 or SUR2, closely related members of the ATP-binding cassette transporter superfamily (Aguilar-Bryan et al., 1995; Inagaki et al., 1995, 1996; Isomoto et al., 1996). In this report, we show that SUR1 and $K_{IR}6.x$ specifically associate to form a stable complex, with an estimated molecular mass of 950 kDa. Formation of this complex is directly correlated with the appearance of K_{ATP} channel activity. Expression of a fusion protein, $SUR1{\sim}K_{IR}6.2$, with a defined 1:1 stoichiometry forms homomeric K_{ATP} channels, also with an estimated molecular mass of 950 kDa. These channels are sensitive to ATP, ADP, sulfonylureas, and diazoxide, showing that a 1:1 stoichiometry is sufficient for channel formation. A triple fusion protein, $SUR1{\sim}(K_{IR}6.2)_2$, forms K_{ATP} channels only if it is coexpressed with monomeric SUR1, indicating that a 1:1 stoichiometry is required for channel formation. The rescue is specific; the triple fusion is not activated by $SUR1_{T1381P(20)X}$, a mutant SUR1 missing the entire second nucleotide binding fold, consistent with a requirement for multiple functional receptors. The results indicate that K_{ATP} channels have a $(SUR/K_{IR}6.x)_4$ stoichiometry.

Results

$K_{IR}6.x$ Is Photolabeled by ^{125}I-Azidoglibenclamide When Expressed with SUR1

SUR1 is labeled covalently with ^{125}I-glibenclamide (Aguilar-Bryan et al., 1990). In addition, the ^{125}I-labeled 4-azidosalicyloyl analog of glibenclamide, ^{125}I-azidoglibenclamide, labels both SUR1 and a 38 kDa protein (Schwanstecher et al., 1994a, 1994b). When cloned channel subunits are coexpressed, ^{125}I-azidoglibenclamide labels both SUR1, $K_{IR}6.2$, and $K_{IR}6.1$, but not $K_{IR}1.1$ (ROMK1) or $K_{IR}3.4$ (GIRK4, CIR, rcKATP-1) (Figure 1A; compare lanes C and E with lanes G and I; the expected molecular masses of $K_{IR}1.1$ and $K_{IR}3.4$ are 45 kDa and 47.8 kDa, respectively). Additional experiments show that labeling of $K_{IR}6.1$ or $K_{IR}6.2$ requires coexpression of SUR1 (data not shown). Immunoblots with anti-$K_{IR}6.2$ antisera confirm the identity of the labeled $K_{IR}6.2$ band (data not shown). Displacement experiments with azidoglibenclamide and glibenclamide indicate that labeling

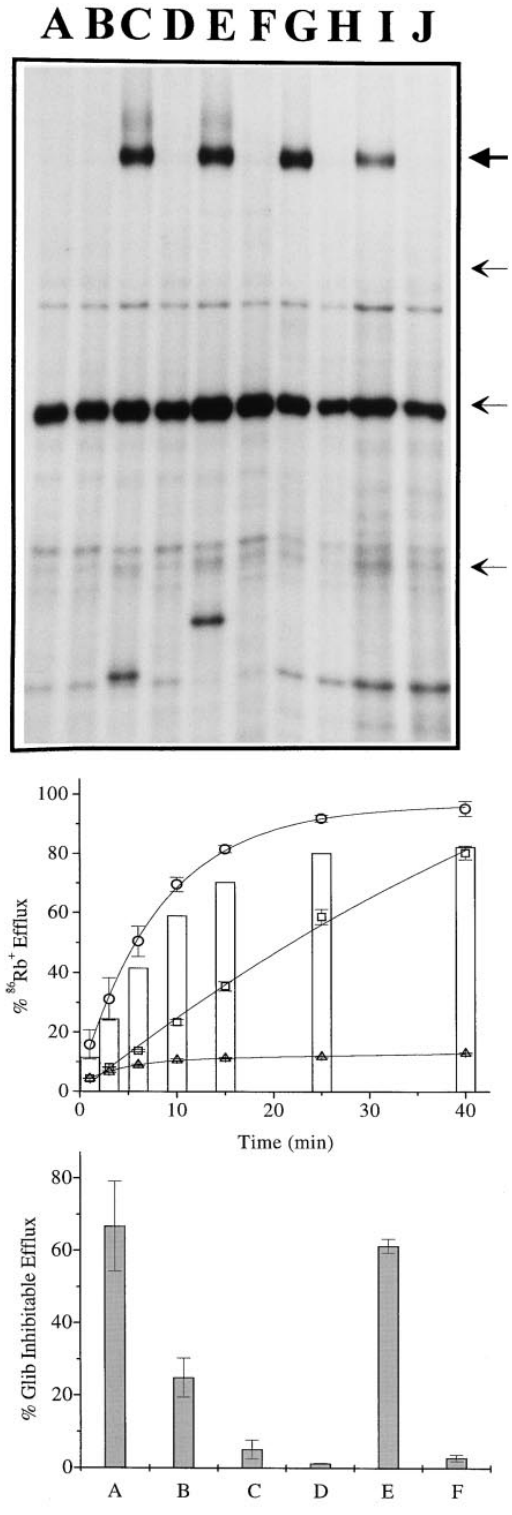

Figure 1. Cophotolabeling of K_{IR} Subunits Correlates with Functional Channels

(A) COSm6 cells expressing SUR1 and K_{IR} subunits were photolabeled with 10 nM ^{125}I-azidoglibenclamide, solubilized in SDS sample buffer, and separated on 7.5% polyacrylamide gels (Laemmli, 1970). Lanes A and B, β-galactosidase controls, minus (A) and plus (B) 1 μM glibenclamide; Lanes C and D, SUR1 + K_{IR}6.2, minus (C) and plus (D) 1 μM glibenclamide; Lanes E and F, SUR1 + K_{IR}6.1, minus (E) and plus (F) 1 μM glibenclamide; Lanes G and H, SUR1 + K_{IR}3.4, minus (G) and plus (H) 1 μM glibenclamide; Lanes I and J, SUR1 + K_{IR}1.1, minus (I) and plus (J) 1 μM glibenclamide. The small arrows represent the positions of MW standards; from the top down, 96 kDa, 68 kDa, and 45 kDa, respectively. The large arrow marks the position of core glycosylated SUR1 at 140 kDa. The prominent band near the middle of the gel is serum albumin.

(B) The $^{86}Rb^+$ efflux assay on COSm6 cells transfected with SUR1 and K_{IR}6.2. Open circles designate efflux from metabolically inhibited cells, open squares indicate basal efflux, and open triangles indicate efflux from cells that are metabolically inhibited and treated with 1 μM glibenclamide to inhibit K_{ATP} channels. The bars show efflux through K_{ATP} channels, termed glibenclamide inhibitable efflux, defined as the difference between the metabolically inhibited and the metabolically inhibited plus glibenclamide values.

(C) Comparison of glibenclamide inhibitable efflux after 40 min from COSm6 cells transfected with SUR1 and the indicated K_{IR} subunits. These experiments have been repeated multiple times, the minimum, n = 2 for SUR1–K_{IR}3.4; the maximum, n > 50 for SUR1–K_{IR}6.2. (A) SUR1 + K_{IR}6.2; (B) SUR1 + K_{IR}6.1; (C) SUR1 + K_{IR}1.1; (D) SUR1 + K_{IR}3.4; and (E) SUR1$_{N\text{-}6X\text{-}HIS}$ + K_{IR}6.2; (F) COS cell control.

of SUR1 and K_{IR}6.2 is lost in parallel, with an estimated K_D of approximately 0.8 nM, as shown previously (Schwanstecher et al., 1994a; Schwanstecher et al., 1994b). The cophotolabeling is specific for the azido derivative and is not observed with ^{125}I-glibenclamide. Cotransfection of SUR1 with K_{IR}6.x leads to the expression of a more highly glycosylated 150–170 kDa species of the receptor, in addition to the core-glycosylated 140 kDa species (Figure 1A; compare lanes C and E with lanes G and I; the large arrow identifies the 140 kDa receptor). The same two species of SUR1 are seen in HIT cells, a clonal β cell line, and have been identified in other cell lines, including the RINm5F β cell line (Nelson et al., 1996) and the αTC-6 glucagon producing cell line (Rajan et al., 1993). This difference in glycosylation between the 140 kDa and the 150–170 kDa species has been described previously (Nelson et al., 1996).

Coexpression of SUR1 and K_{IR}6.x generates K_{ATP} channel activity, detectable by $^{86}Rb^+$ efflux techniques and single channel recording. Figure 1B illustrates the $^{86}Rb^+$ efflux assay using SUR1 and K_{IR}6.2. Efflux through K_{ATP} channels (bars), termed % Glib Inhibitable Efflux, is defined as the difference between the efflux determined with metabolically inhibited cells in which K_{ATP} channels are activated, and the efflux determined with metabolically inhibited cells in which K_{ATP} channels are simultaneously blocked with 1 μM glibenclamide. As shown previously, COSm6 cells have an endogenous $^{86}Rb^+$ efflux that is inactivated by metabolic inhibition (Inagaki et al., 1995). Inactivation of this endogenous efflux, and inactivation of K_{ATP} channel activity with glibenclamide, result in the low level of efflux shown in Figure 1B (open triangles). Cotransfection of K_{IR}6.1 with SUR1 also generated K_{ATP} channel activity at ~35% of the amount seen with K_{IR}6.2. Neither K_{IR}1.1 nor K_{IR}3.4 produced a significant glibenclamide-sensitive change in $^{86}Rb^+$ efflux when cotransfected with SUR1, as compared with COS cell controls (Figure 1C). The formation of active K_{ATP} channels is thus correlated with changes in the glycosylation pattern of SUR1 and with cophotolabeling of K_{IR}6.x.

His-Tagged SUR1 Forms K_{ATP} Channels and Complexes with K_{IR}6.x

A 6X-histidine tag was introduced onto the N-terminus of SURI to aid purification. Based upon the predicted

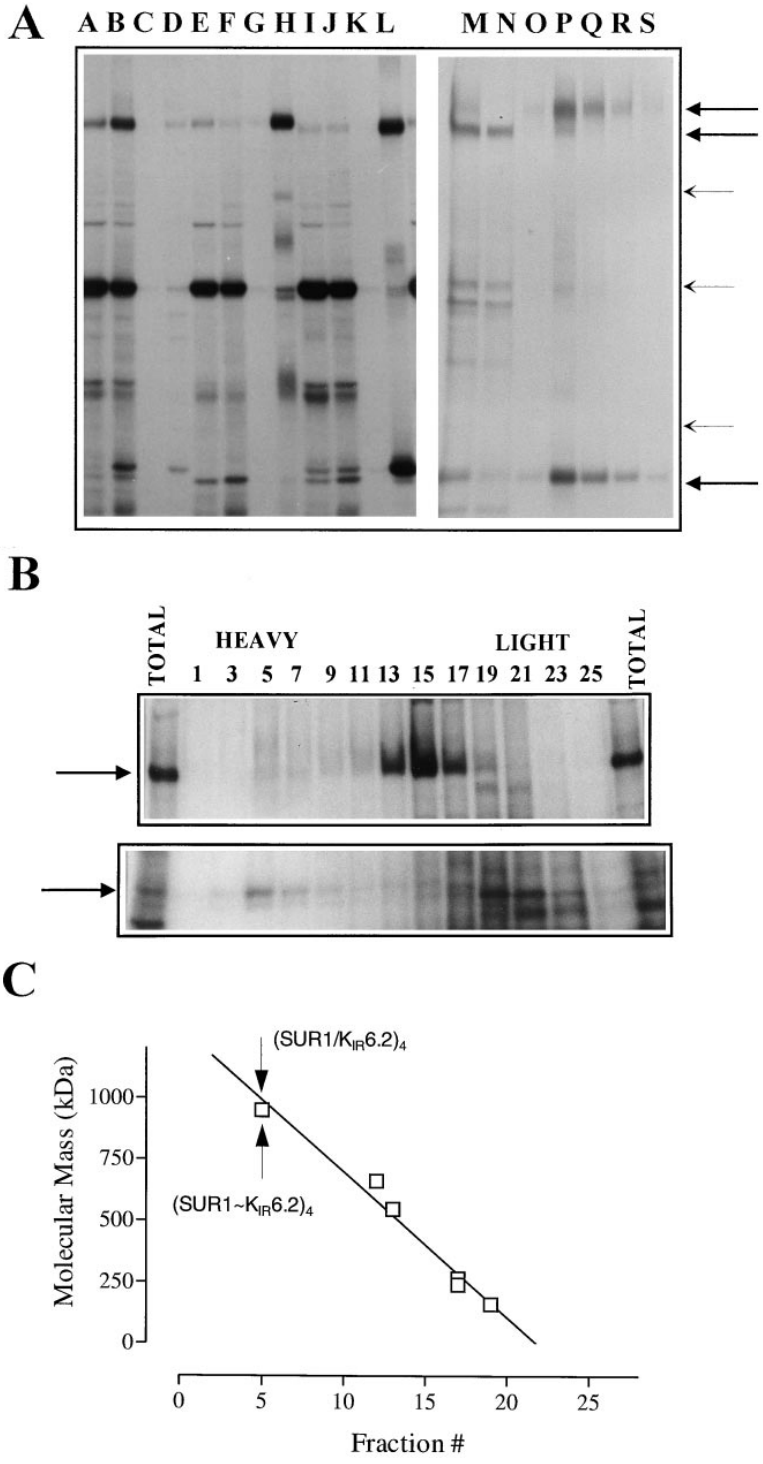

Figure 2. SUR1 and K_{IR}6.2 Associate to Form Large Multimeric Complexes

(A) Copurification of SUR1 and K_{IR}6.2 after prelabeling transfected cell membranes with ^{125}I-azidoglibenclamide and solubilization in digitonin. Lanes A–D show the starting sample, run-through, wash, and 0.1 M imidazole eluate from a Ni^{2+}–agarose column loaded with SUR1, not his-tagged, and K_{IR}6.2. Lanes E–H show the same fractionation using his-tagged SUR1 alone. Lanes I–L show the results using his-tagged SUR1 plus K_{IR}6.2. Lanes M–S illustrate fractionation on wheat germ agglutinin–agarose. Lane M shows the starting sample, and lane N is the unbound fraction, while lanes O–S are fractions eluted with N-acetylglucosamine.

(B) Fractionation of SUR1–K_{IR}6.2 complexes on sucrose gradients. The upper section shows photolabeling in the high molecular weight region with SUR1 marked with an arrow; the lower section shows a lower molecular weight region with K_{IR}6.2 marked with an arrow.

(C) Estimate of the molecular mass of the highly glycosylated SUR1–K_{IR}6.2 complex. The largest unfused complex is marked by a down arrow; the position of the fused complex is the same (up arrow). The protein markers employed were aldolase (160 kDa), catalase (240 kDa), urease (trimer = 272 kDa; hexamer = 545 kDa), thyroglobulin (660 kDa), and pentameric IgM (950 kDa).

transmembrane topology of SUR1, the histidine tag should be extracellular, with the sequence MHHHHHHM, where the second M is the natural start site of SUR1. $SUR1_{N\text{-}6X\text{-}HIS}$–$K_{IR}$6.2 channels are active (Figure 1C), and additional experiments show that they are activated by diazoxide and have single channel properties equivalent to native SUR1–K_{IR}6.2 channels. $SUR1_{N\text{-}6X\text{-}HIS}$ and K_{IR}6.2 are cophotolabeled by ^{125}I-azidoglibenclamide (10 nM), to the same degree as wild-type SUR1 and K_{IR}6.2 (Figure 2A). The association of $SUR1_{N\text{-}6X\text{-}HIS}$ with K_{IR}6.2 was demonstrated by digitonin solubilization of membranes from COSm6 cells coexpressing both subunits, followed by Ni^{2+}–agarose chromatography (Figure 2A; compare lanes A–D with lanes I–L). Analogous experiments show that $SUR1_{N\text{-}6X\text{-}HIS}$ also forms stable complexes with K_{IR}6.1 (data not shown). The complexes of wild-type SUR1

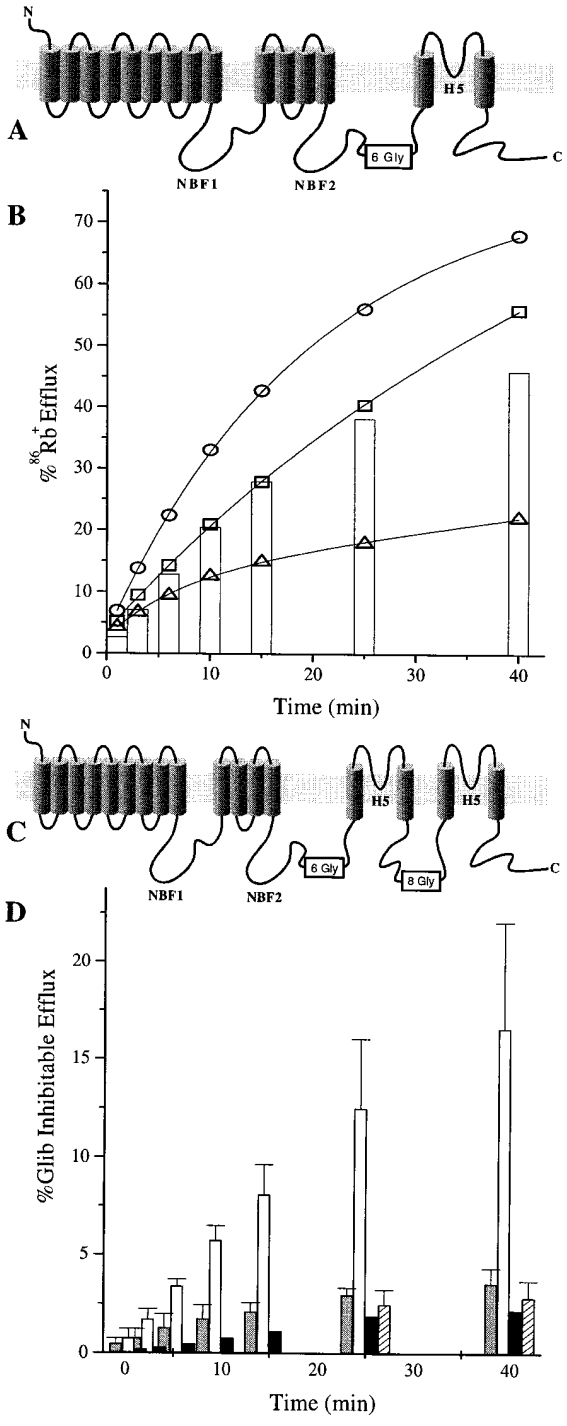

Figure 3. SUR1–K_{IR}6.2 Fusions Can Form Active K_{ATP} Channels

(A and C) Illustrations of the fusion constructs used. SUR1 and K_{IR}6.2 were fused tail–head through a six glycine linker to produce SUR1∼K_{IR}6.2. The triple fusion, SUR1∼(K_{IR}6.2)$_2$, was constructed by fusing an additional K_{IR}6.2 subunit through an eight glycine linker to SUR1∼K_{IR}6.2.

(B) The $^{86}Rb^{+}$ efflux assay on COSm6 cells transfected with SUR1∼K_{IR}6.2 shows active channels. The percentage of total $^{86}Rb^{+}$ efflux is plotted. Open circles indicate flux from metabolically inhibited cells, open squares indicate basal efflux, and open triangles indicate efflux from metabolically and glibenclamide inhibited cells.

(D) Glibenclamide inhibitable $^{86}Rb^{+}$ efflux from COSm6 cells transfected with triple fusion constructs. Cells transfected with the triple fusion construct alone (shaded bars, n = 3) show only background efflux, comparable to that seen from untransfected COSm6 cells. Cotransfection with SUR1∼(K_{IR}6.2)$_2$ and monomeric SUR1 (open bars, n = 4) indicate the triple fusion protein can be rescued by monomeric SUR1 but not with a truncated SUR1, SUR1$_{T1381P(20)X}$, missing the second nucleotide binding fold (black bars, n = 1). For lack of space, only two untransfected COSm6 cell controls are shown at 25 and 40 min (lined bars, n = 4).

and K_{IR}6.2, with no his-tag, show minimal binding to Ni^{2+}–agarose (Figure 2, lanes A–D). The nonspecific binding observed (Figure 2; compare lane D with lane L) is due to the fact that we have chosen not to include a low concentration of imidazole or histidine in the wash buffer. SUR1$_{N\text{-}6X\text{-}HIS}$ alone shows no labeled bands at the position of either K_{IR}6.1 or K_{IR}6.2, indicating that there is no coupling with possible endogenous COSm6 cell K_{IR} subunits.

SUR1$_{N\text{-}6X\text{-}HIS}$ and K_{IR}6.x are associated, but fractionation on Ni^{2+}–agarose does not distinguish between the two glycosylated forms of the receptor. Figure 2A, lanes M–S, illustrates the fractionation of SUR1–K_{IR}6.2 complexes on wheat germ agglutinin–agarose. The starting sample contains both the 140 kDa and the 150–170 kDa species (Figure 2A, lane M). The 140 kDa form is not adsorbed to wheat germ, while the 150–170 kDa species is completely adsorbed. The bulk of the labeled material at the K_{IR}6.2 position is adsorbed to wheat germ, although K_{IR}6.2 has no consensus glycosylation site. Additional experiments show that the apparent molecular mass of the K_{IR}6.2 band is not altered by growing transfected cells in tunicamycin, which eliminates glycosylation of SUR1 (Nelson et al., 1996). The 150–170 kDa species and K_{IR}6.2 are eluted with N-acetylglucosamine. Note also that there is some lower molecular mass material trailing the 150–170 kDa band, suggesting either incorporation of some 140 kDa receptor into complexes or incorporation of receptors that have been processed partially to the more highly glycosylated form. The results of fractionation on Ni^{2+}– and wheat germ agglutinin–agarose indicate that SUR1 and K_{IR}6.2 interact, and that the majority of the K_{IR}6.2 is associated with the complex glycosylated 150–170 kDa species of the receptor. Additional experiments showed that the complexes isolated from wheat germ agglutinin–agarose could be concentrated and fractionated on a Sephadex S400 gel filtration column, and that SUR1 and K_{IR}6.2 coelute as a large complex (data not shown).

The Molecular Weight of the Highly Glycosylated SUR1–K_{IR}6.2 Complexes Is Consistent with an Octameric K_{ATP} Channel, (SUR1–K_{IR}6.2)$_4$

The molecular mass of the digitonin stable complexes was determined by sedimentation velocity measurements in sucrose gradients. The 140 kDa species appears to be polydisperse, with estimated molecular masses ranging from 300–500 kDa (compare Figure 2B, lanes 13–17, with molecular mass standards in Figure 2C). The K_{IR} region on the gel is contaminated with other labeled proteins, and it is unclear how much K_{IR}6.2 is associated with the 140 kDa receptor complexes. The

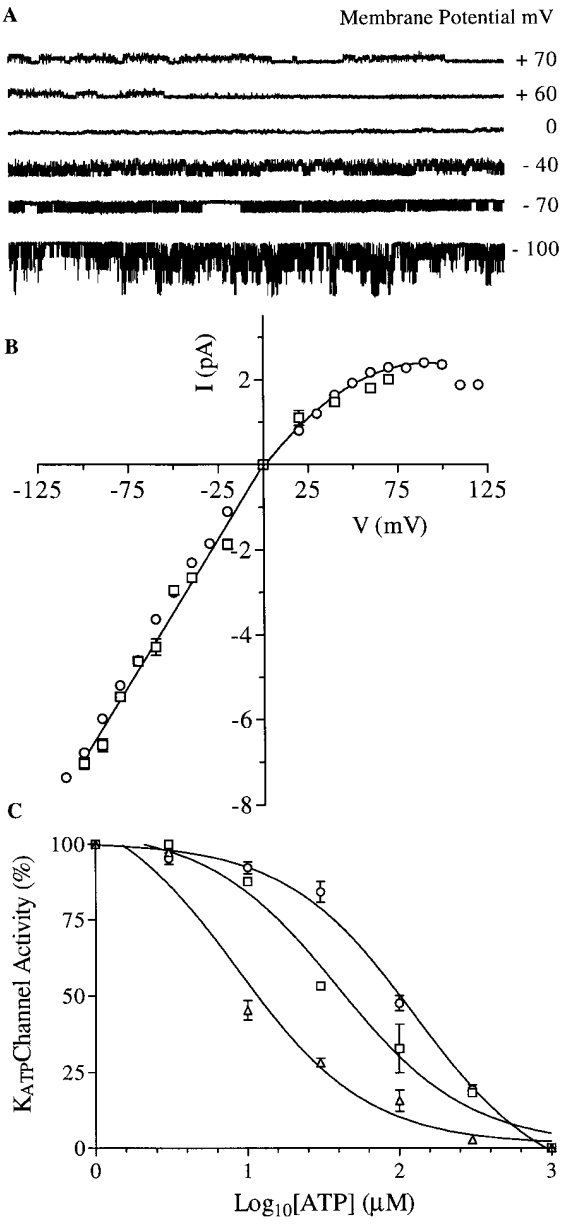

Figure 4. Electrophysiology of the Fusion Channels

(A) Representative traces from COSm6 cells expressing SUR1∼K_{IR}6.2 channels. Recordings were made in the inside-out patch-clamp configuration in symmetrical 140 mM K^+, at the indicated holding potentials.

(B) The current–voltage curves for SUR1∼K_{IR}6.2 (open squares) and SUR1∼$(K_{IR}6.2)_2$ + SUR1 (open circles) channels are indistinguishable. Both channels show weak inward rectification at potentials positive to EK with a conductance of 69 pS ± 3 pS, identical to that of unfused SUR1–K_{IR}6.2 channels (solid line).

(C) ATP dose-response curves for SUR1–K_{IR}6.2 (open triangles), SUR1∼K_{IR}6.2 (open squares), and SUR1∼$(K_{IR}6.2)_2$ + SUR1 (open circles) K_{ATP} channels. The half-maximal values for inhibition are 8.5, 35, and 114 μM, respectively.

150–170 kDa species associates with K_{IR}6.2 to make complexes that cosediment with IgM pentamers at 950 kDa (compare Figure 2B, lane 5, with Figure 2C markers), consistent with the formation of an octameric channel.

Fusion Proteins with Defined Stoichiometries Form Active K_{ATP} Channels

SUR1∼K_{IR}6.2 Channels

The genes encoding SUR1 and K_{IR}6.2 are clustered on human chromosome 11, with the last exon of SUR1 4.5kB upstream of the intronless K_{IR}6.2 gene (Inagaki et al., 1995; Aguilar-Bryan and Bryan, 1996). This positioning suggested that these genes may have been fused at an earlier evolutionary time and prompted construction of SUR1∼K_{IR}6.2, a fusion of SUR1 and K_{IR}6.2, to test whether a 1:1 stoichiometry was sufficient to make active channels. The predicted topology of the fusion protein is shown in Figure 3A; the C-terminus of SUR1 is joined to the N-terminus of K_{IR}6.2 through six glycine residues, with 15 predicted transmembrane spanning helices and a defined 1:1 ratio of SUR1:K_{IR}6.2. SUR1∼K_{IR}6.2 is expressed in COSm6 cells, can be photolabeled with 10 nM ^{125}I-azidoglibenclamide, and has an estimated size, by SDS–PAGE, of approximately 190 kDa (calculated MW = 220 kDa). Expression of SUR1∼K_{IR}6.2 in COSm6 cells generates functional ATP-sensitive, potassium selective channels that are activated by metabolic poisoning, as shown by $^{86}Rb^+$ efflux experiments (Figure 3B). Efflux was inhibited by glibenclamide (half maximal at 26 nM, versus 1.8 nM for wild type; Hill coefficient = 0.5, versus 1.2 for wild type) and activated by diazoxide (100 μM). In symmetrical 140 mM potassium, the fusion channels show mild inward rectification in the presence of 2 mM magnesium, with a reversal potential near 0 mV (Figure 4B). The estimated conductance is 69 pS ± 1 pS at a membrane potential of −60 mV. Representative recordings are shown in Figure 4A. The channels are completely inhibited by 1 mM ATP and activated by 500 μM MgADP in the presence of 100 μM ATP. The SUR1∼K_{IR}6.2 channels were ∼5-fold less sensitive to ATP (EC_{50} = 41 μM, versus 8.9 μM) than unfused SUR1–K_{IR}6.2 channels (Figure 4C).

The molecular mass of the ^{125}I-azidoglibenclamide labeled fusion protein complex was determined by solubilization of transfected COSm6 cell membranes in 1% digitonin, followed by sucrose gradient centrifugation. The large labeled complexes of SUR1∼K_{IR}6.2 cosedimented with the large SUR1–K_{IR}6.2 complexes, with an estimated molecular mass of 950 kDa (Figure 2C; arrow).

SUR1∼$(K_{IR}6.2)_2$ + SUR1 Channels

To determine whether a 1:1 ratio of channel subunits was required to form functional K_{ATP} channels, a triple fusion protein, SUR1∼$(K_{IR}6.2)_2$, was engineered (Figure 3C). Metabolic inhibition of COSm6 cells expressing the triple fusion protein did not activate $^{86}Rb^+$ efflux significantly (Figure 3D, compare shaded bars with striped bars). Cotransfection of the triple fusion construct with a plasmid expressing the green fluorescence protein (GFP) (Chalfie et al., 1994; Marshall et al., 1995) was used to identify transfected cells for single channel recording. Eighteen of twenty patches on fluorescence cells transfected with SUR1∼$(K_{IR}6.2)_2$ had no K_{ATP} channel activity, while two of twenty patches showed a short-lived current (<30 s) that was not characterized further. Cotransfection of the triple fusion construct with monomeric SUR1 rescued channel activity. Twenty of twenty patches showed ATP-sensitive K^+ channels. $^{86}Rb^+$ efflux was activated by metabolic inhibition of cells transfected with SUR1∼$(K_{IR}6.2)_2$ + SUR1, and was inhibited

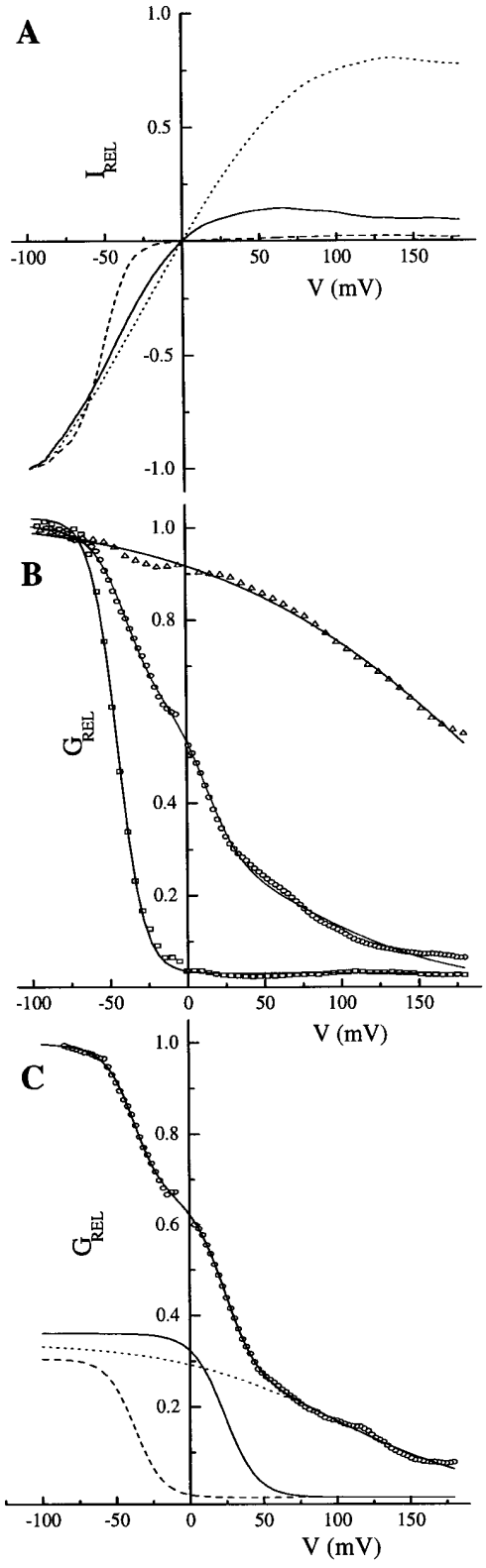

Figure 5. Mixtures of Strong and Weak Rectifying Triple Fusion Channels Give Rise to Three Channel Species When Cotransfected with Monomeric SUR1

(A) Current–voltage (I–V) relationships, (B) relative conductance–voltage data (G_{REL}–V), and (C) estimated components from mixed expression. The dashed lines in each panel are for the strong rectifier case (SUR1∼$(K_{IR}6.2_{N160D})_2$ + SUR1), the solid lines are for the mixed case (SUR1∼$(K_{IR}6.2)_2$ + SUR1∼$(K_{IR}6.2_{N160D})_2$ + SUR1), and the dotted lines are for the weak rectifier case (SUR1∼$(K_{IR}6.2)_2$ + SUR1). In (B) and (C), every 20th data point is shown for the strong (open squares), mixed (open circles), and weak (open triangles) rectifier cases, while the lines are derived from fits of the entire data set to either a single Boltzmann function (strong and weak rectifier cases) or the sum of three Boltzmann functions (mixed cases). (C) illustrates the three individual Boltzmann components that model the measured conductance. The data in (A) and (B) were obtained using 100 μM spermine, and should be compared with that in (C) obtained using 10 μM spermine.

by 1 μM glibenclamide (Figure 3D, compare shaded bars with open bars). The I–V data for the SUR1∼$(K_{IR}6.2)_2$ + SUR1 channels can be superimposed on the SUR1–$K_{IR}6.2$ and SUR1∼$K_{IR}6.2$ channel results. All exhibit mild inward rectification and a 69 pS ± 3 pS conductance in symmetrical 140 mM KCl at −60 mV (Figure 4B). The rescued triple fusion channels require higher [ATP] than SUR1∼$K_{IR}6.2$ to inhibit channel activity (EC_{50} = 110 μM versus 41 μM; Figure 4C). Expression of SUR1 alone does not produce K_{ATP} channels (Inagaki et al., 1995); thus, we assume that the coexpression of SUR1 restores a required 1:1 ratio of SUR1:$K_{IR}6.2$.

As rescue of the triple fusion protein required monomeric SUR1, we tested whether a functional receptor was necessary. $SUR1_{T1381P(20)X}$, a C-terminal truncation of SUR1 that parallels the behavior of two receptor mutations that cause familial hyperinsulinism (Dunne et al., 1997), was tested for its ability to rescue the triple fusion protein. This receptor is truncated at the second Walker A motif, is expressed in COSm6 cells, and can be photolabeled by ^{125}I-azidoglibenclamide, but it does not form active K_{ATP} channels when cotransfected with $K_{IR}6.2$ (Dunne et al., 1997). Coexpression of $SUR1_{T1381P(20)X}$ with SUR1∼$(K_{IR}6.2)_2$ does not rescue channel activity, implying that four functional receptors are required for activation of the pore (Figure 3D, black bars).

Active Triple Fusion Channels Have a Tetrameric Pore

The K_{ATP} channels formed by SUR1 and $K_{IR}6.2$ show weak inward rectification in the presence of polyamines but can be converted to strong rectifiers by changing a single residue in the permeation path, aspargine 160 in the second transmembrane spanning domain (M2), to aspartate (Shyng et al., 1997). Mixtures of strong and weak inward rectifiers have been used to estimate the number of subunits in channels (Glowatzki et al., 1995). Cotransfection of SUR1 with equal amounts of $K_{IR}6.2$ and $K_{IR}6.2_{N160D}$ give rise to hetero-oligomeric channels, whose relative conductance–voltage (G–V) curves are best fit by the sum of five Boltzmann functions, consistent with four $K_{IR}6.2$ subunits generating the potassium pore (Shyng et al., 1997). We have analyzed the voltage dependence of spermine block (Glowatzki et al., 1995) in mixtures of weak and strongly rectifying triple fusion channels. Coexpression and SUR1 rescue of a mixture of triple fusion constructs, SUR1∼$(K_{IR}6.2_{N160D})_2$ and SUR1∼$(K_{IR}6.2)_2$, yields three classes of channels as expected from a tetrameric pore. The parental weak and

strong rectifiers are recovered along with an intermediate, heterologous species. The results of one experiment are summarized in Figure 5, which shows the I–V and derived G–V data. K_{ATP} channels formed by cotransfection of SUR1 and SUR1∼$(K_{IR}6.2_{N160D})_2$ are strongly rectifying and have a relative G–V curve that is well fit by a single Boltzmann function (Figure 5B, open squares and dashed line). SUR1 plus SUR1∼$(K_{IR}6.2)_2$ channels show weak inward rectification with a shallow G–V curve that is also well fit by a single Boltzmann function (Figure 5B, open triangles and dotted line). Cotransfection of equimolar amounts of SUR1, SUR1∼$(K_{IR}6.2_{N160D})_2$, and SUR1∼$(K_{IR}6.2)_2$ give rise to an additional species of channel as seen in the G–V data and the fit of three summed Boltzmann functions (Figure 5B, open circles and solid line). Based on χ^2 analysis, less acceptable fits were obtained with the sum of either two or four Boltzmann functions. Figure 5C shows the relative values of the three species obtained from the fitting procedure. The conductances depend on the concentration of spermine used. The conductance curves shift to lower voltages and become somewhat steeper as the spermine concentration is increased. Compare the data for the mixed transfection in Figure 5B (open circles), where the spermine concentration is 100 μM, with the data in Figure 5C, where the spermine concentration is 10 μM. Simple random association predicts a 0.25:0.50:0.25 ratio of the three channel species starting with a 1:1 mixture. The estimated ratios from the experiment in Figure 5C, 0.30:0.36:0.34, suggest that the wild-type triple fusion protein was more abundant in this patch. The results clearly show formation of the heterologous channel type (solid line = mixed, in Figure 5C: n = 5 experiments). These results imply that four $K_{IR}6.2$ subunits associate to form the potassium selective pore and that four SUR1 subunits are required for expression of full K_{ATP} channel activity.

Discussion

ATP-sensitive potassium channels are a unique family composed of a sulfonylurea receptor, SUR, a member of the ATP-binding cassette superfamily, and $K_{IR}6.x$, a member of the inward rectifier potassium channel family. Neither subunit alone exhibits channel activity; both are essential. The pancreatic β cell channel is comprised of SUR1, the high affinity sulfonylurea receptor and $K_{IR}6.2$ (Inagaki et al., 1995; Aguilar-Bryan and Bryan, 1996). SUR2A and B, receptors with lower affinities for sulfonylureas, combine with $K_{IR}6.2$ to form channels with properties similar to the K_{ATP} channels found in heart and vascular smooth muscle (Inagaki et al., 1996; Isomoto et al., 1996). A mutation, N160D, in the M2 segment of $K_{IR}6.2$ has been used to identify it as part of the permeation pathway. This mutation alters the conductance properties of the β cell channel from weak to strong rectification. In other members of the inward rectifier potassium channel family, it has been concluded that the analogous residue forms part of the channel pore and forms a binding site for Mg^{2+} and polyamines that are required for rectification (Lu and MacKinnon, 1994; Fakler et al., 1994; Wible et al., 1994; Yang, 1995; Lopatin et al., 1995a, 1995b). The results indicate that the M2 segment of $K_{IR}6.2$ probably contributes to the permeation pathway and imply that, like other inward rectifier potassium channels (Glowatzki et al., 1995; Yang et al., 1995), the pore is tetrameric.

Direct Interactions between SUR1 and $K_{IR}6.2$

The range of possible associations of ABC proteins with channel subunits is unknown. On the basis of a possible mechanism for regulation of outwardly rectifying chloride channels by CFTR, SUR and other ABC proteins were proposed to be separate from channel subunits (Al-Awqati, 1995). Several lines of evidence, presented here, show that SUR1 and $K_{IR}6.2$ are associated and form detergent stable complexes. First, SUR1 and $K_{IR}6.x$ cophotolabel with ^{125}I-azidoglibenclamide, although only SUR1 binds the sulfonylurea with high affinity (K_D = 0.8 nM) (Schwanstecher et al., 1994a, 1994b). Second, coexpression of $K_{IR}6.x$ with SUR1 alters the glycosylation state of the receptor. Expression of SUR1 alone produces a core-glycosylated, 140 kDa receptor that can be purified on concanavalin A, while coexpression with $K_{IR}6.x$ also produces a higher molecular mass species, 150–170 kDa, which is retained on wheat germ agglutinin–agarose, indicating more complex glycosylation with the addition of sialic acid. Both the 140 kDa and 150–170 kDa species are found in β cell models and other cell lines. The core-glycosylated species is the major form in HIT cell membranes, while the two forms are about equally abundant in RINm5F cells and αTC-6 cells (Nelson et al., 1996). Third, $K_{IR}6.2$ copurifies with SUR1 on Ni^{2+}–agarose (histidine-tagged SUR1) or wheat germ agglutinin–agarose. The wheat germ agglutinin results indicate that $K_{IR}6.2$ is preferentially associated with the 150–170 kDa form of SUR1. Fourth, estimates of the molecular mass of the SUR1–$K_{IR}6.2$ complex (950 kDa, see Figure 2) are consistent with an octameric, (SUR1–$K_{IR}6.2)_4$ channel.

SUR1–$K_{IR}6.x$ complex formation is specific and correlates with the appearance of K_{ATP} channel activity. SUR1 and $K_{IR}6.1$ or $K_{IR}6.2$ associate to produce K_{ATP} channels; $K_{IR}1.1$ (ROMK1) and $K_{IR}3.4$ (rcKATP, CIR) did not associate with SUR1, and no K_{ATP} channel activity was found when these subunits were coexpressed in COS cells. These results are different from those reported by Ämmälä et al. (1996), who described "promiscuous" coupling of SUR1 with ROMK1 and possibly other K_{IR}s in HEK293 cells. The reasons for the different results are unclear.

The finding that association with $K_{IR}6.x$ affects the glycosylation of SUR1 suggests that SUR1 and $K_{IR}6.2$ associate in the endoplasmic reticulum before transit to the Golgi, since complex glycosylation is usually considered to occur in the medial Golgi. We typically see an excess of the 140 kDa core-glycosylated receptor under the transfection conditions used and speculate that efficient glycosylation and transit of SUR1 to the plasma membrane requires association with $K_{IR}6.2$. Ozanne et al. (1995) have reported that the 140 kDa protein is localized to intracellular membranes, while the 150–170 kDa species is in the plasma membrane in insulinoma cells. The results support the conclusion that the complex

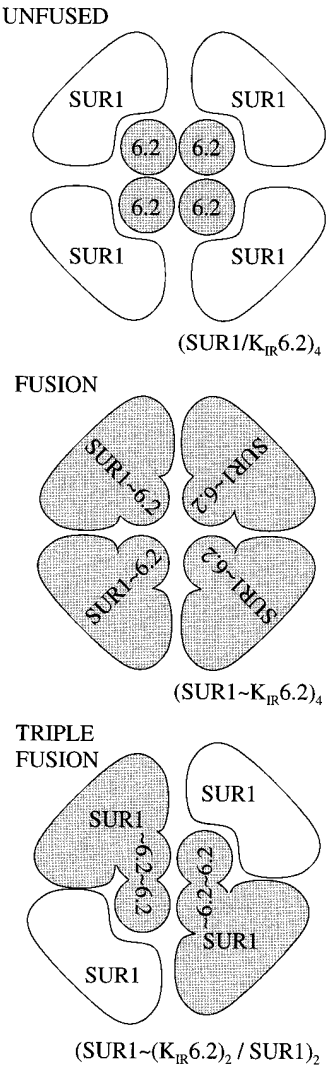

Figure 6. Diagram Illustrating the Proposed Tetrameric Architecture of the Unfused, Fused, and Triple Fusion ATP-Sensitive Potassium Channels

glycosylated receptor is in active K_{ATP} channels on the cell surface.

Stoichiometry of K_{ATP} Channels

The data indicate that active β cell K_{ATP} channels are octameric with a (SUR1–K_{IR}6.2)$_4$ stoichiometry. Cophotolabeling of K_{IR}6.2 implied a close proximity of at least one channel subunit to SUR1. Labeling of the 150–170 kDa species of SUR1 and K_{IR}6.2 in the partially purified complexes (Figure 2, lane P) appeared to be of comparable intensity; however, this does not provide an index of stoichiometry since the relative efficiencies of subunit labeling are not known. The molecular mass estimate, 950 kDa, of the large complexes formed by K_{IR}6.2 and the 150–170 kDa form of SUR1 are consistent with an octamer having a calculated protein mass of $4 \times (177{,}000 + 43{,}000) = 880{,}000$ daltons, plus additional mass due to glycosylation. However, various other SUR1:K_{IR}6.2 stoichiometries could account for the 950 kDa complex.

We engineered fusion constructs of SUR1 with K_{IR}6.2 to determine whether a 1:1 SUR1:K_{IR}6.2 stoichiometry is necessary and sufficient for the assembly of active K_{ATP} channels. Fusion of the N-terminus of K_{IR}6.2 to the C-terminus of SUR1 through a glycine linker generated a fusion protein with 15 predicted transmembrane spanning domains and a defined 1:1 SUR1:K_{IR}6.2 stoichiometry. Expression of SUR1∼K_{IR}6.2 produced weakly rectifying, K^+ selective conductances with properties similar to those of the SUR1–K_{IR}6.2 channels. The SUR1∼K_{IR}6.2 channels are less sensitive to inhibition by ATP and glibenclamide; furthermore, the concentration-response curves for ATP and glibenclamide showed altered Hill coefficients. The detailed reasons for these differences are not clear but presumably result from the restricted mobility of the subunit ends. We speculate that the formation of functional channels by these fusion proteins implies that the C- and N-termini of SUR1 and K_{IR}6.2, respectively, are in close proximity in the native channel and may interact to transmit nucleotide and sulfonylurea-induced conformational changes in SUR1 to the pore. Fusion of the two polypeptides clearly could be expected to affect this transmission. Overall, the results show that a 1:1 SUR1:K_{IR}6.2 stoichiometry is sufficient to assemble functional K_{ATP} channels with the same molecular mass as unfused channels.

A head–tail triple fusion, SUR1∼(K_{IR}6.2)$_2$, was engineered by adding a second inward rectifier subunit to SUR1∼K_{IR}6.2. This construct specifies a protein with 17 predicted transmembrane spanning domains and a defined 1:2 SUR1:K_{IR}6.2 stoichiometry. Transfection of COSm6 cells with the triple fusion construct did not generate functional K_{ATP} channels detectable either by activation of $^{86}Rb^+$ efflux following metabolic inhibition or by single channel recording. Importantly, the triple fusion channels could be "rescued" by coexpression with monomeric SUR1. Our interpretation is that monomeric SUR1 restores the 1:1 stoichiometry, which is required for the assembly of functional channels. The triple fusion channels are activated by metabolic inhibition, exhibit weak rectification identical to that seen with SUR1–K_{IR}6.2 and SUR1∼K_{IR}6.2 channels, and have reduced sensitivity to inhibition by ATP and glibenclamide.

Together with the mass estimate of 950 kDa, the rescue of the triple fusion channel by monomeric SUR1 implied that active K_{ATP} channels have a (SUR1–K_{IR}6.2)$_4$ stoichiometry. To support this conclusion further, we engineered a triple fusion construct with the $K_{IR}6.2_{N160D}$ subunit that shows strong rectification. Expressed alone, this construct does not produce active channels but is rescued by monomeric SUR1 and generates strongly rectifying channels. More importantly, when mixtures of SUR1∼(K_{IR}6.2)$_2$ and SUR1∼($K_{IR}6.2_{N160D}$)$_2$ are rescued by monomeric SUR1, a channel with intermediate rectification properties is observed, showing that both the strongly and weakly rectifying subunits must participate in forming the pore.

The results are summarized in Figure 6, which illustrates the overall architecture and proposed stoichiometries of the K_{ATP} channels discussed. Copurification of K_{IR}6.x with SUR1 indicates direct association of

K_{ATP} subunits. $K_{IR}6.2$ is identified as forming the permeation pathway because the N160D mutation in M2 affects the rectification properties of the channel. Expression of a fusion protein, SUR1∼$K_{IR}6.2$, demonstrated that a 1:1 stoichiometry was sufficient to produce K_{ATP} channels, while expression of a triple fusion protein, SUR1∼$(K_{IR}6.2)_2$, failed to produce channels but could be rescued by coexpression with monomeric SUR1, implying that a 1:1 stoichiometry was necessary for channel formation. Coexpression of triple fusion proteins, SUR1∼$(K_{IR}6.2)_2$ and SUR1∼$(K_{IR}6.2_{N160D})_2$, produced one intermediate conductance in addition to the strongly and weakly rectifying species, demonstrating that both the wild-type and N160D subunits must participate in formation of the intermediate conductance channel. Finally, determination of the molecular mass of the SUR1–$K_{IR}6.2$ complex, 950 kDa, directly confirms an $(SUR1–K_{IR}6.2)_4$ architecture and supports the view that the receptors in a functional K_{ATP} channel are complex glycosylated. We speculate that SUR2–$K_{IR}6.x$ channels will have an equivalent architecture.

Experimental Procedures

Plasmids

To generate *pECE–SUR1$_{N\text{-}6X\text{-}HIS}$*, the 3′ *EcoRI* and *SacI* sites of the hamster SUR1 cDNA (pECE–haSUR1) (Inagaki et al., 1995) were deleted by two rounds of partial cleavage, blunt ending with Klenow, and religation. PCR primers were designed to amplify a specific fragment to introduce a histidine tag. The forward primer reads 5′-GTC AGA ATT CGC CGC CAT GCA TCA CCA TCA CCA TCA CAT GCC CTT GGC CTT CTG CG-3′ and contains an internal *EcoRI* site, a Kozak consensus sequence (Kozak, 1987), a start codon, and codons encoding six tandem histidine residues followed by a 5′ SUR1 cDNA sequence. The reverse primer reads 5′-GCT GTG GTG GAT GTG CAC C-3′. The two primers amplify an approximately 250 bp sequence, when pECE–SUR1 is used as a template. The 250 bp product was cleaved with *EcoRI* and *SacI* and ligated into identically digested pECE–haSUR1. The resultant constructs were sequenced to confirm introduction of the tag and to eliminate possible PCR artifacts.

The fusion constructs were made as follows: $K_{IR}6.2$ was cloned into the 3′ *EcoRI* site of pECE–haSUR1 to create *pECE–haSUR1–K$_{IR}$6.2*. The two coding sequences were then fused using PCR overlap extension. In the first PCR reaction, haSUR1 forward primer, 5′-CCA GCA GAA GCT CTA GAA TAT ACC-3′, and fusion reverse primer, 5′-GCC CTT TCG GGA CAG CAT ACC TCC ACC TCC ACC TCC CTT GTC CGC ACG GAC AAA-3′, generated a 1.2 kb fragment, using haSUR1 as a template. In a second PCR reaction, $K_{IR}6.2$ reverse primer, 5′-GAG TGG ATG CTG GTG ACA CA-3′, and fusion reverse primer, 5′-TTT GTC CGT GCG GAC AAG GGA GGT GGA GGT GGA GGT ATG CTG TCC CGA AAG GGC-3′, generated a 600 bp fragment, using $K_{IR}6.2$ as a template. These two fragments were gel purified and combined in a third overlap PCR reaction, using the haSUR1 forward primer and the $K_{IR}6.2$ reverse primer. The resulting 1.8 kb fragment was digested with *NotI* and *XhoI* restriction enzymes and ligated into identically cut pECE–haSUR1–$K_{IR}6.2$. The resulting pECE–SUR1∼$K_{IR}6.2$ fusion was sequenced to confirm the fusion, as well as to check PCR fidelity. To create *pECE–haSUR1∼(K$_{IR}$6.2)$_2$*, the first $K_{IR}6.2$ subunit was synthesized using PCR and the forward primer, 5′-GTA CGA ATT CGC CGC CAT GCT GTC CCG AAA GGG C-3′, with the reverse primer, 5′-CTA CTC TAG ACT AAT CGA TAC CTC CAC CTC CAC CTC CAC CTC CGG ACA AGG AAT CTG GAG-3′, using pECE–$K_{IR}6.2$ as a template. The resulting 1.2 kb fragment was digested with *XbaI* and *EcoRI* (sites in primers) and ligated into pECE. This construct, pECE–$K_{IR}6.2_{8Gly}$, introduced eight glycine residues followed by an isoleucine and an aspartic acid residue (coding a *ClaI* site in the primer), before termination at the C-terminus. The second $K_{IR}6.2$ subunit was synthesized also using PCR and the forward primer, 5′-GTC AAT CGA TAT GCT GTC CCG AAA GGG C-3′, with the reverse primer, 5′-CTA CTC TAG ACT ACA TAT GGG ACC AGG AAT CTG GAG A-3′, using pECE–$K_{IR}6.2$ as a template. The resulting 1.2 kb fragment was digested with *ClaI* and *XbaI* (sites in the primers) and ligated into pECE–$K_{IR}6.28$Gly, cut identically. This generated the dimeric $K_{IR}6.2$ construct, pECE–$K_{IR}6.28$Gly-$K_{IR}6.2$, which was tested for and found to have K_{ATP} channel activity when expressed with SUR1 (data not shown). A 5 kb fragment from pECE–SUR1∼$K_{IR}6.2$ was then made by digestion with *EcoRI* and *XhoI*. This fragment was cloned into a 5 kb fragment generated by digestion of pECE–$K_{IR}6.2_{8Gly}$-$K_{IR}6.2$ with *EcoRI* and followed by partial digestion with *XhoI*. Ligation of these two fragments created the triple fusion, pECE–SUR1∼$(K_{IR}6.2)_2$, where SUR1 and the first $K_{IR}6.2$ are linked by six Gly residues and the two $K_{IR}6.2$ moieties are separated by a linker encoding –Gly_8–Ile–Asp–. To check PCR fidelity, each $K_{IR}6.2$ subunit was then individually subcloned into either the pECE or pCMV expression vector and cotransfected with SUR1. Both $K_{IR}6.2$ constructs individually were capable of forming K_{ATP} channels. pECE–SUR1$(K_{IR}6.2_{N160D})_2$ was created in an identical fashion using pECE–$K_{IR}6.2_{N160D}$.

Cell Culture and Transfections

COSm6 cells were plated at a density of 1×10^6 per dish (150 mm diameter) and cultured in DMEM HG (high glucose), supplemented with 10% fetal calf serum. Transfections were done as follows. For $^{86}Rb^+$ efflux studies, 3-day-old cultures of COSm6 cells were trypsinized and replated at a density of 2.0×10^5 cells per 35 mm well (six-well dish) and allowed to attach overnight. Typically, 5 μg of a SUR1 plasmid was mixed with 5 μg of a K_{IR} plasmid and brought up to 7.5 μl final volume in TBS (8 g/l NaCl; 0.38 g/l KCl; 0.2 g/l Na_2HPO_4; 3.0 g/l Tris base; 0.15 g/l $CaCl_2$; and 0.1 g/l $MgCl_2$ [pH 7.5]) before addition of DEAE–dextran (30 μl of a 5 mg/ml solution in TBS). The samples were vortexed, collected by briefly spinning in a microfuge, then incubated for 15 min at room temperature before addition of 500 μl 10% NuSerum in TBS. Cells were washed twice with Hank's balanced salt solution (HBSS), the DNA mix was added, and the cells were maintained in a 37°C CO_2 incubator. After 4 hr, the DNA mix was decanted, and the cells were shocked for 2 min in 1 ml HBSS + 10% DMSO, then placed in 1.5 ml of DMEM HG + 2% FBS + 10 μM chloroquine and kept in a 37°C CO_2 incubator. After 4 hr, the cells were washed twice with HBSS and incubated in normal growth media until assayed (usually 36–48 hr posttransfection).

Rubidium Efflux Assays

Between 24 and 36 hr posttransfection, cells were placed in fresh media containing approximately 1 μCi/ml ^{86}RbCl for 12–24 hr and assayed as follows. Cells were incubated for 30 min at 25°C in Krebs' Ringer solution under one of three conditions: no additions (basal), with oligomycin (2.5 μg/ml) and 2-deoxy-D-glucose (1 mM) (metabolically inhibited), or with oligomycin and deoxyglucose plus 1 μM glibenclamide (K_{ATP} channels inhibited). Cells were washed once in $^{86}Rb^+$-free Krebs' Ringer solution, with or without the added inhibitors, and then time points were taken by removing all the medium from the cells and replacing it with fresh medium at the indicated times. Equal portions of the medium from each time point were counted, and the values were summed to determine flux. Total $^{86}Rb^+$ is defined as the sum of counts from each time point plus the counts released by addition of 1% SDS to the cells. As indicated, the data are presented either as the percentage of total cellular $^{86}Rb^+$ released or as % glibenclamide inhibitable efflux. The latter measure represents specific K_{ATP} channel activity and is defined as the difference between $\%^{86}Rb^+$ efflux from metabolically inhibited cells versus $\%^{86}Rb^+$ efflux from metabolically inhibited plus glibenclamide (efflux through K_{ATP} channels = % glibenclamide inhibitable efflux ≡ % metabolically inhibited efflux − % metabolically and glibenclamide inhibited efflux).

Membrane Preparation

COSm6 cells were transfected for membrane preparations as described above, with the following modifications. Cells were plated at a density of 1.5×10^6 cells per 100 mm dish. K_{IR} plasmid (100 μg) was added to 100 μg of SUR1 plasmid, and the mixture was used to transfect ten 100 mm plates. The DNA mix was brought up

to 500 μl with TBS, and 2 ml of DEAE–dextran (5 mg/ml) was added. The mixture was vortexed and allowed to incubate for 30 min at room temperature. Twenty-eight milliliters of 10% NuSerum in TBS was added to the DNA mix, and 3 ml of this mixture was added to each 100 mm plate for 4 hr. The transfections were carried out as above, except that 5 ml was the operating volume for each 100 mm plate. Membranes were prepared 60–72 hr posttransfection from 10–20 100 mm dishes. Transfected cells were washed twice in phosphate-buffered saline (PBS) (pH 7.4), then scraped in PBS and collected in 10 ml plastic tubes. The cells were pelleted, resuspended in 10 ml of hypotonic buffer (5 mM Tris–HCl [pH 7.4] and 2 mM EDTA), and allowed to swell for 45 min on ice. Cells were then homogenized, transferred to a 15 ml glass tube, and spun at 1000 g for 20 min at 4°C to remove nuclei and unbroken cells. The supernatant was then transferred to a polycarbonate centrifuge tube, and membranes were collected by ultracentrifugation at 40,000 rpm in an 80Ti fixed angle rotor for 2 hr. The pelleted membranes were resuspended in 300 μl of membrane buffer (50 mM Tris–HCl [pH 7.4] and 5 mM EDTA) and stored at −80°C. Typical protein concentrations are 2–5 mg/ml.

Photolabeling

Photolabeling was carried out as described for isolated membranes (Aguilar-Bryan et al., 1990; Nelson et al., 1992) or using live cells. Living cells, grown in six-well dishes, were washed three times with PBS, then incubated in the dark with 10 nM ^{125}I-azidoglibenclamide (Schwanstecher et al., 1994a) or 10 nM ^{125}I-iodoglibenclamide (Aguilar-Bryan et al., 1990), in Krebs' Ringer solution supplemented with 10 mM glucose. After 30 min at room temperature, the cells were irradiated in an ultraviolet cross-linker (Model FB-UVXL-1000, Spectronics Corp., Westbury, NY) at a setting of 9×10^5 mJ/cm^2. Excess unbound drug was removed by three 5 ml washes with PBS (1 min each). The cells were then solubilized in 250–500 μl of 2× SDS sample buffer (Laemmli, 1970). Aliquots were separated on 8% polyacrylamide gels, stained with Coomassie Blue, dried, and autoradiographed (Nelson et al., 1992). Isolated membranes, 5–20 μg, were incubated in 50 mM MES (pH 6.5) containing 10 nM ^{125}I-glibenclamide or ^{125}I-azidoglibenclamide. After 30 min at room temperature, the mix was irradiated and solubilized in an equal amount of 2× SDS sample buffer. Aliquots were separated on 5%–8% polyacrylamide gels, depending on the molecular size of interest; stained, dried, and autoradiographed.

Chromatography

$SUR1_{N\text{-}6X\text{-}HIS}$–$K_{IR}6.x$ complexes were partially purified by chromatography on a 500 μl column of Ni^{2+}–agarose (Quiagen Corp.) equilibrated in solubilization buffer (1.0% digitonin, 150 mM NaCl, and 25 mM Tris [pH 7.4]) plus 4 mM imidazole (pH 7.4). Approximately 150 μg of membranes prepared from COSm6 cells transfected with the appropriate inward rectifier and SUR1 plasmids were photolabeled with 10 nM ^{125}I-azidoglibenclamide (pH 6.5). The labeled membranes were then solubilized in 200 μl of solubilization buffer for 30 min on ice, then spun for 30 min at 100,000 g (Model TI-100, Beckman Instruments) to remove insoluble material, and passed over the Ni^{2+} column four times. The column was washed with 20 ml (40 × column volume) of 0.2% digitonin wash buffer, then eluted with wash buffer containing 100 mM imidazole (pH 7.4). Aliquots of each fraction were analyzed by PAGE, as described above. Complexes were separated on wheat germ agglutinin–agarose, as described by Nelson et al. (1996).

Sucrose Gradients

Membranes from transfected cells were isolated, photolabeled with ^{125}I-azidoglibenclamide, and solubilized as described previously. Twelve milliliters of 5%:20% linear sucrose gradients (in 0.1% digitonin, 100 mM NaCl, and 50 mM Tris [pH 7.4]) were poured in SW41 tubes using a Biocomp Gradient Master 106. The solubilized proteins were loaded on top of the gradient and sedimented at 36,000 rpm in a SW-41Ti rotor, using a Beckman L8–80M ultracentrifuge for 9 hr at 4°C. Fractions (0.5 ml) were collected using a Bio-Rad model 2110 fraction collector. A portion of each fraction (70 μl) was combined with 15 μl 2-mercaptoethanol and 25 μl of 5× SDS sample buffer. A portion of this mixture (100 μl) was separated on a 1.5 mm thick 7.5% polyacrylamide gel. Gels were stained, dried, and visualized by autoradiography. The markers used were: IgM (950 kDa), thyroglobulin (660 kDa), urease (hexamer = 545 kDa), urease (trimer = 272 kDa), catalase (240 kDa), and aldolase (160 kDa).

Patch-Clamp Recording

After transfection, the cells were cultured for 48–72 hr. Single channel recordings were made in the transfected cells in the inside-out patch orientation. The intracellular solution contained 140 mM KCl, 2 mM $MgSO_4$, 0.084 mM $CaCl_2$, 1 mM EGTA, and 10 mM HEPES (pH 7.2). Na_2ATP (1 μM) was added to the intracellular solution unless otherwise noted. Recordings were made at room temperature (20–22°C). Patch electrodes (5–7 Gigaohm) with fire-polished tips were prepared. The pipette solution contained 140 mM KCl, 2 mM $CaCl_2$, and 10 mM HEPES (pH 7.4). Channel activity was measured at a holding potential of −60 mV using an amplifier (Axopatch-1C, Axon Instruments, Foster City, CA) and monitored on a high gain oscilloscope (V-660 Hitachi, Japan). Data were stored to tape using a digital data recorder (VR-10, Instrutech Corp., New York). Currents were filtered at 2 kHz and digitized at 20 kHz for analysis. Inward currents are shown as downward deflections.

Current–voltage relationships (I–V curves) were constructed by measuring single channel current amplitudes at different membrane potentials. All amplitude histograms were carried out with 20–30 s of recording to determine the unitary currents at different voltages. Alternatively, currents were recorded from macro patches containing many channels. For comparison, the I–V data in Figure 5A, obtained from macro patches, were normalized to the individual current values at −100 mV.

ATP dose-response curves were obtained for each inside-out patch for different concentrations of ATP (1–1000 μM). Current (I) was measured as a fraction of the mean current (I_c) obtained in control solutions (with 1 μM ATP). The relative (I/I_c) current was plotted against the concentration of ATP. The dose-response curve was drawn by fitting the data to a Hill equation, using a nonlinear least squares method. The value for half-maximal inhibition (IC_{50}) of K_{ATP} channel activity was obtained from the following equation:

$$I/I_c = \frac{1}{\left(1 + \left(\frac{[L]}{IC50}\right)^n\right)}$$

where [L] is the concentration of ATP, and n is the Hill coefficient.

The voltage dependence of spermine block was analyzed using a modification of the procedure described by Glowatzki et al. (1995) as follows. A patch was pulled, then moved into intracellular solution containing spermine (0, 1, 10, or 100 μM). The holding potential was ramped from 0 to +180 mV, held for 30 ms to allow spermine to enter the pore, then ramped, 0.68 mV/ms, to −100 mV. The current (I) was sampled every 0.2 ms during the ramp. Ten I–V recordings were averaged. The solution was switched to intracellular solution with spermine plus 5 mM ATP to close K_{ATP} channels, and the protocol was repeated. Residual capacitative currents were removed by subtracting the averaged ATP data from the non-ATP data. Conductance (G) values were calculated by dividing each current (I) value by the corresponding driving force ($V\text{-}E_K$; $E_K = 0$ in symmetrical potassium). Relative conductance values ($G_{REL} \equiv G_{SPM}/G_0$) were then calculated by dividing the conductance values in the presence of spermine, G_{SPM}, by the conductance values in the absence of spermine, G_0, at each voltage. Spikes in the conductance data around the reversal potential (=0 mV), typically a 3–5 mV range, were not included in the fitting process. Boltzmann functions,

$$G_{REL} = \sum_i A_i/(1 + e^{(v - v_{1/2})/v_S})$$

were fit to the G_{REL}–V data using Origin 4.1 (Microcal, Inc., Northampton, MA). $V_{1/2}$ is the voltage for half-maximal block by spermine; V_S is the voltage required for an e-fold change in conductance of species i having amplitude A_i. In Figure 5, every 20th data point is shown, but the complete data sets, except as noted at the reversal potentials, were used in the fitting process.

Acknowledgments

Antibodies against $K_{IR}6.2$ and plasmids encoding $K_{IR}6.1$ and $K_{IR}6.2$ were generously provided by Susumu Seino. GIRK4 was kindly provided by David Clapham. ROMK1 was kindly provided by Kevin Ho. Margarita Lopez and Li-Zhen Song provided expert technical assistance. This work was funded by NIH, JDF, and ADA grants to J. B. and L. A. B. and by a grant from the Houston Endowment to L. A. B.

Received January 15, 1997; revised March 21, 1997.

References

Aguilar-Bryan, L., and Bryan, J. (1996). ATP-sensitive potassium channels, sulfonylurea receptors and persistent hyperinsulinemic hypoglycemia of infancy. Diabetes Rev. *4*, 336–346.

Aguilar-Bryan, L., Nelson, D.A., Vu, Q.A., Humphrey, M.B., and Boyd A.E., III (1990). Photoaffinity labeling and partial purification of the beta cell sulfonylurea receptor using a novel, biologically active glyburide analog. J. Biol. Chem. *265*, 8218–8224.

Aguilar-Bryan, L., Nichols, C.G., Wechsler, S.W., Clement, J.P., IV, Boyd, A.E., III, Gonzalez, G., Herrera-Sosa, H., Nguy, K., Bryan, J., and Nelson, D.A. (1995). Cloning of the beta cell high-affinity sulfonylurea receptor: a regulator of insulin secretion. Science *268*, 423–426.

Al-Awqati, Q. (1995). Regulation of ion channels by ABC transporters that secrete ATP (Perspective). Science *269*, 805–806.

Ämmälä, C., Moorhouse, A., Gribble, F., Ashfield, R., Proks, P., Smith, P.A., Sakura, H., Coles, B., Ashcroft, S.J., and Ashcroft, F.M. (1996). Promiscuous coupling between the sulphonylurea receptor and inwardly rectifying potassium channels. Nature *379*, 545–548.

Ashcroft, F.M. (1988). Adenosine 5′-triphosphate-sensitive potassium channels. Annu. Rev. Neurosci. *11*, 97–118.

Chalfie, M., Tu, Y., Euskirchen, G., Ward, W., and Prasher, D. (1994). Green fluorescent protein as a marker for gene expression. Science *263*, 802–805.

Dunne, M.J., Kane, C., Shepherd, R.M., Sanchez, J.A., James, R.F.L., Johnson, P.R.V., Aynsley-Green, A., Lu, S., Clement, J.P., IV, Lindley, K.J., Seino, S., and Aguilar-Bryan, L. (1997). Familial persistant hyperinsulinemic hypoglycemia of infancy and mutations in the sulfonylurea receptor. N. Engl. J. Med. *336*, 703–706.

Fakler, B., Brandle, U., Bond, C., Glowatzki, E., Konig, C., Adelman, J.P., Zenner, H.P., and Ruppersberg, J.P. (1994). A structural determinant of differential sensitivity of cloned inward rectifier K^+ channels to intracellular spermine. FEBS Lett. *356*, 199–203.

Glaser, B., Chiu, K.C., Anker, R., Nestorowicz, A., Landau, H., Ben, B.H., Shlomai, Z., Kaiser, N., Thornton, P.S., Stanley, C.A., et al. (1994). Familial hyperinsulinism maps to chromosome 11p14–15.1, 30 cM centromeric to the insulin gene. Nature Genet. *7*, 185–188.

Glowatzki, E., Fakler, G., Brandle, U., Rexhausen, U., Zenner, H.P., Ruppersberg, J.P., and Fakler, B. (1995). Subunit-dependent assembly of inward-rectifier K^+ channels. Proc. R. Soc. Lond. (B) *261*, 251–261.

Inagaki, N., Gonoi, T., Clement, J.P., IV, Namba, N., Inazawa, J., Gonzalez, G., Aguilar-Bryan, L., Seino, S., and Bryan, J. (1995). Reconstitution of I_{KATP}: an inward rectifier subunit plus the sulfonylurea receptor. Science *270*, 1166–1170.

Inagaki, N., Gonoi, T., Clement, J.P., Wang, C.Z., Aguilar-Bryan, L., Bryan, J., and Seino, S. (1996). A family of sulfonylurea receptors determines the pharmacological properties of ATP-sensitive K^+ channels. Neuron *16*, 1011–1017.

Isomoto, S., Kondo, C., Yamada, M., Matsumoto, S., Higashiguchi, O., Horio, Y., Matsuzawa, Y., and Kurachi, Y. (1996). A novel sulfonylurea receptor forms with BIR (Kir6.2) a smooth muscle type ATP-sensitive K^+ channel. J. Biol. Chem. *271*, 24321–24324.

Kane, C., Shepherd, R.M., Squires, P.E., Johnson, P.R., James, R.F., Milla, P.J., Aynsley-Green, A., Lindley, K.J., and Dunne, M.J. (1996). Loss of functional K_{ATP} channels in pancreatic beta-cells causes persistent hyperinsulinemic hypoglycemia of infancy. Nature Med. *2*, 1344–1347.

Kozak, M. (1987). An analysis of 5′-noncoding sequences from 699 vertebrate messenger RNAs. Nucleic Acids Res. *15*, 8125–8148.

Laemmli, U.K. (1970). Cleavage of structural proteins during the assembly of the head of bacteriophage T4. Nature *227*, 680–685.

Lopatin, A.N., Makhina, E.N., and Nichols, C.G. (1995a). The mechanism of inward rectification of potassium channels: "long-pore plugging" by cytoplasmic polyamines. J. Gen. Physiol. *106*, 923–955.

Lopatin, A.N., Makhina, E.N., and Nichols, C.G. (1995b). Potassium channel block by cytoplasmic polyamines as the mechanism of intrinsic rectification. Nature *372*, 366–369.

Lu, Z., and MacKinnon, R. (1994). Electrostatic tuning of Mg^{2+} affinity in an inward-rectifier K^+ channel. Nature *371*, 243–246.

Marshall, J., Molloy, R., Moss, G., Howe, J., and Hughes, T. (1995). The jellyfish green fluorescent protein: a new tool for studying ion channel expression and function. Neuron *14*, 211–215.

Misler, S., Falke, L.C., Gillis, K., and McDaniel, M.L. (1986). A metabolite-regulated potassium channel in rat pancreatic B cells. Proc. Natl. Acad. Sci. USA *83*, 7119–7123.

Nelson, D.A., Aguilar-Bryan, L., and Bryan, J. (1992). Specificity of photolabeling of beta-cell membrane proteins with an ^{125}I-labeled glyburide analog. J. Biol. Chem. *267*, 14928–14933.

Nelson, D.A., Bryan, J., Wechsler, S., Clement, J.P., IV, and Aguilar-Bryan, L. (1996). The high affinity sulfonylurea receptor: distribution, glycosylation, purification, and immunoprecipitation of two forms from endocrine and neuroendocrine cell lines. Biochemistry *35*, 14793–14799.

Nestorowicz, A., Clement, J.P., IV, Wilson, B.A., Schoor, K.P., Hiroshi, I., Glaser, B., Landau, H., Stanley, C., Thornton, P.S., Bryan, J., Aguilar-Bryan, L., and Permutt, M.A. (1996a). Mutations in the sulfonylurea receptor gene are associated with familial hyperinsulinism in Ashkenazi Jews. Hum. Mol. Genet. *5*, 1813–1822.

Nestorowicz, A., Schoor, K.P., Wilson, B.A., Glaser, B., Seino, S., and Permutt, M.A. (1996b). Identification of a non-sense mutation in the β cell inward rectifier, BIR, associated with familial hyperinsulinism, p. 748. Proceedings of the 10th International Congress of Endocrinology, San Francisco, CA.

Noma, A. (1983). ATP-regulated K^+ channels in cardiac muscle. Nature *305*, 147–148.

Ozanne, S.E., Guest, P.C., Hutton, J.C., and Hales, C.N. (1995). Intracellular localization and molecular heterogeneity of the sulphonylurea receptor in insulin-secreting cells. Diabetologia *38*, 277–282.

Rajan, A.S., Aguilar-Bryan, L., Nelson, D.A., Nichols, C.G., Wechsler, S.W., Lechago, J., and Bryan, J. (1993). Sulfonylurea receptors and ATP-sensitive K^+ channels in clonal pancreatic alpha cells. Evidence for two high affinity sulfonylurea receptors. J. Biol. Chem. *268*, 15221–15228.

Schwanstecher, M., Loser, S., Chudziak, F., Bachmann, C., and Panten, U. (1994a). Photoaffinity labeling of the cerebral sulfonylurea receptor using a novel radioiodinated azidoglibenclamide analogue. J. Neurochem. *63*, 698–708.

Schwanstecher, M., Loser, S., Chudziak, F., and Panten, U. (1994b). Identification of a 38-kDa high affinity sulfonylurea-binding peptide in insulin-secreting cells and cerebral cortex. J. Biol. Chem. *269*, 17768–17771.

Shyng, S.L., Clement, J.P., IV, Bryan, J., and Nichols, C.G. (1997). Stoichiometry of the K_{ATP} channel complex. Biophys. J. *72*, A251.

Thomas, P.M., Cote, G.J., Hallman, D.M., and Mathew, P.M. (1995a). Homozygosity mapping of the gene for familial persistent hyperinsulinemic hypoglycemia of infancy to chromosome 11p. Am. J. Hum. Genet. *56*, 416–421.

Thomas, P.M., Cote, G.J., Wohlik, N., Haddad, B., Mathew, P.M., Rabl, W., Aguilar-Bryan, L., Gagel, R.F., and Bryan, J. (1995b). Mutations in the sulfonylurea receptor gene in familial hyperinsulinemic hypoglycemia of infancy. Science *268*, 426–429.

Thomas, P., Ye, Y., and Lightner, E. (1996). Mutations of the pancreatic islet inward rectifier also lead to familial persistent hyperinsulinemic hypoglycemia of infancy. Hum. Mol. Gen. *5*, 1809–1812.

Wible, B.A., Taglialatela, M., Ficker, E., and Brown, A.M. (1994). Gating of inwardly rectifying K^+ channels localized to a single negatively charged residue. Nature *371*, 246–249.

Yang, J., Jan, Y.N., and Jan, L.Y. (1995). Control of rectification and permeation by residues in two distinct domains in an inward rectifier K^+ channel. Neuron *14*, 1047–1054.